Aerodynamic Simulation of NACA 0012 Airfoil at Low Angles of Attack Using CFD

MUHAMMAD RASHID IQBAL[1], SANA MARRYAM[2]
[1, 2]*Department of Mathematics and statistics, Institute of Southern Punjab University Multan, Pakistan*

Abstract- ***The NACA four-digit classification system defines airfoil geometry through a four-part code. Maximum camber (first digit, % of chord), camber position (second digit, tenths of chord), and maximum thickness (last two digits, % of chord) are specified. Notably, a 12% maximum thickness indicates a symmetric airfoil profile with no camber. This study examines the aerodynamic performance of a NACA 0012 airfoil under subsonic flow conditions. We analyze the behavior of the airfoil in terms of the lift it produces as a result of air attacking it. We calculate lift against a C-type geometry. The mathematical model considers varying angles of attack for values of inlet velocity. The mathematical model includes the Nervier-Stokes equations and the Standard k turbulence model to capture the turbulence. The model involves solving a set of nonlinear partial equations and differential equations simultaneously. The finite volume method serves as the solver for this task. ANSYS Workbench 16.2 includes FLUENT for solving all simulations.***

Indexed Terms- ***NACA0012 Airfoil, Lift and Drag Coefficient, Angle of attack, Numerical Analysis, CFD, ANSYS Fluent.***

I. INTRODUCTION

Aircraft operating at low speeds, particularly during takeoff and landing, demand elevated lift forces to counteract weight. Traditional aircraft designs exhibit maximum lift coefficients (C_L max) around 1.4-1.5 [1]. Enhancing C_L max is crucial for reducing stall speed. However, increasing wing surface area, although effective, introduces additional drag. High lift devices provide a solution by dynamically altering airfoil characteristics to optimize C_L max during low-speed flight regimes. Singh (2017) [2] investigated the aerodynamic implications of plain flap deployment on NACA 66-01 airfoils. Findings indicated stall angle increments and performance enhancements at elevated angles of attack. Increased flap deflection resulted in expanded flow trapping beneath the airfoil, concomitantly reducing flow velocity and augmenting pressure. Simultaneously, intensified adverse pressure gradients provoked heightened flow separation. Computational validation was achieved via FLUENT ANSYS analysis. Katz and Largman (2016) [3] explored the aerodynamic characteristics of a two-element airfoil incorporating a 900 trailing edge flap. Results showed the flap, extending 5% beyond chord length, markedly enhanced lift over diverse angles of attack. Although maximum lift coefficient increased, lift to drag ratio decreased. Mahmood et al. (1995) [4] employed a dual experimental-numerical approach to investigate airflow behavior around the high lift NACA 4412 airfoil, considering both flap equipped and flap-less configurations. Experimental efforts targeted the airflow above the airfoil, highlighting the trailing-edge separation region. Abdelrahman et al. (2020) [5] focused on optimizing flap configuration to minimize detrimental effects. Results showed that trailing edge flaps augment lift coefficients; however, they also introduce unfavorable flow circulation and pressure gradients, highlighting the need for careful design consideration.

The aerodynamic characteristics of the NACA 0012 wing, specifically its curved profile, result in decreased drag and mitigated shock wave intensity. These attributes directly affect aircraft maneuverability and lift production, contributing to improved flight performance [6]. Hsiun and Chen (1996) [7] applied a finite volume method with k-ε turbulence modeling to an NACA 4412 airfoil, incorporating a fixed ground boundary. Results showed reduced lift in extreme ground effect due to boundary layer formation. Barber et al. (1998) [8] explored the influence of ground boundary conditions on NACA 4412 airfoil aerodynamics. Findings indicated that fixed ground conditions are unsuitable for WIG applications, leading to the recommendation

of a moving ground boundary aligned with free stream velocity. Chun and Chang (2003) [9] employed finite difference methods and Baldwin-Lomax turbulence closure to examine the influence of ground condition variability on NACA 4412 airfoil aerodynamics, highlighting substantial disparities between fixed and moving grounds. Research employing moving ground boundary conditions has consistently shown lift increments during ground-effect flight, despite variations in force prediction accuracy. Notably, viscous solvers have facilitated in depth analyses of three dimensional WIG configurations, as demonstrated by Hirata and Hino (1997) and Wu and Rozhdestvensky (2001) [10]. Belamadi, R. et al.'s [11] investigation into slot effects on wind turbine airfoil aerodynamics demonstrated improved performance with optimized slot positioning and dimensions. Notably, slots yielded significant benefits at moderate to high angles of attack (10°-20°). Research by Beyhaghi, S. et al. [12] revealed that integrating two segment slots into the NACA 4412 airfoil yields a substantial enhancement in lift coefficient, with an average increase of 8% observed across all angles of attack. Research by Almusawi, M. et al. [13] utilized CFD simulations with k-ω turbulence closure to assess the aerodynamic influence of a spanwise semicircular groove on NACA0012 airfoil performance. Findings indicated significant improvements, with the groove enhancing lift efficiency by 2.25% and reducing drag coefficient by 4.32% under consistent 20 m/s flow conditions. Research by Almusawi, M. et al. [13] utilized CFD simulations with k-ω turbulence closure to assess the aerodynamic influence of a spanwise semicircular groove on NACA0012 airfoil performance. Findings indicated significant improvements, with the groove enhancing lift efficiency by 2.25% and reducing drag coefficient by 4.32% under consistent 20 m/s flow conditions.

The objective behind this study is to reduce lift and drag in the NACA 0012 airfoil. We position a device to regulate the airfoil's lift and drag separation. The CFD program ANSYSFLUENT 16.2, the best configuration not only reduces lift and drag but also increases the lift to drag ratio.

II. MATHEMATICAL MODELING

The continuity equation for a two-dimensional, steady, and incompressible flow is as follows:

$$\frac{\partial \mu}{\partial x}+\frac{\partial v}{\partial y}=0 \quad (1)$$

The momentum equations for viscous flow in the x and y directions are as follows:

$$\rho\left(\frac{\partial \mu}{\partial t}+\mu\frac{\partial \mu}{\partial x}+v\frac{\partial \mu}{\partial y}\right)=-\frac{\partial \rho}{\partial x}+\rho\delta_x+\mu\left(\frac{\partial^2 \mu}{\partial x^2}+\frac{\partial^2 \mu}{\partial y^2}\right) \quad (2)$$

$$\rho\left(\frac{\partial v}{\partial t}+\mu\frac{\partial v}{\partial x}+v\frac{\partial v}{\partial y}\right)=-\frac{\partial \rho}{\partial x}+\rho\delta_y+\mu\left(\frac{\partial^2 v}{\partial x^2}+\frac{\partial^2 v}{\partial y^2}\right) \quad (3)$$

2.1 Turbulence Model

We use Standard k-ϵ turbulence models for capturing the turbulence in the flow. This model contains two transport equations which are simultaneously solved with the flow model. These equations are

$$\frac{\partial}{\partial t}(\rho k)+\frac{\partial}{\partial x_i}(\rho k \mu_t)=\frac{\partial}{\partial x_i}\left[\mu+\left(\frac{\mu_t}{\sigma_k}\right)\frac{\partial k}{\partial x_i}\right]+G_k+G_b-\rho\in-Y_M+S_k \quad (4)$$

$$\frac{\partial}{\partial t}(\rho k)+\frac{\partial}{\partial x_i}(\rho\in \mu_t)=\frac{\partial}{\partial x_i}\left[\mu+\left(\frac{\mu_t}{\sigma_\epsilon}\right)\frac{\partial}{\partial x_i}\right]+C_{1\epsilon}\frac{\in}{k}(G_b)-C_{2\epsilon}\rho\frac{\in^2}{k}+S_\epsilon \quad (5)$$

2.2 Geometry

NACA 0012 airfoil coordinate point with a 100mm chord ware obtained from the Airfoil tools database. The coordinate point ware imported into ANSYS CFD software to generate the NACA 0012 airfoil model (see the fig. 1.)

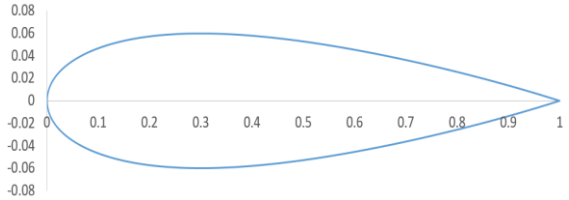

Fig. 1: NACA 0012 geometry

2.3 Domain setup

We imported the 2D NACA0012 model from ANSYSFLUENT and set the computational fluid domain dimension to the chord line, which is the symmetry profile of the NACA0012 airfoil (see Fig. 2). The computational domain for our computations is C-type geometry, with radius circular arcs 5m representing the velocity inlet and pressure outlet, and horizontal lines is 6m attached to the outlet as symmetry lines. The airfoil body is a solid boundary, not part of the domain.

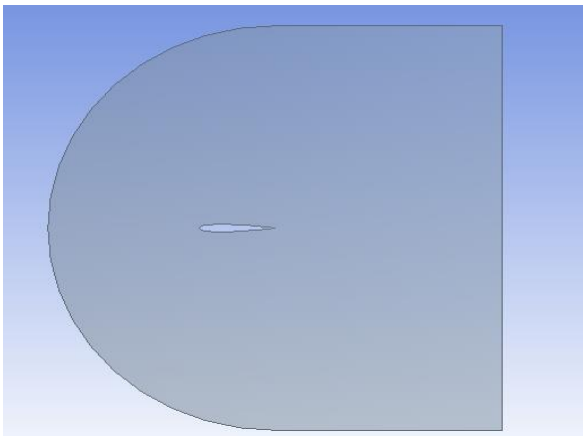

Fig. 2. C-Type Geometry NACA0012

2.4 Meshing

In order to use the finite volume method, the computational domain must be discretized into smaller volumes. In our computational mesh, there are 24426 nodes and 47790 elements with an average skewness of 0.062032, an average aspect ratio of 1.2167, and an average orthogonal quality of 0.96215.An isometric view and Airfoil design are shown in Fig. 3, respectively.

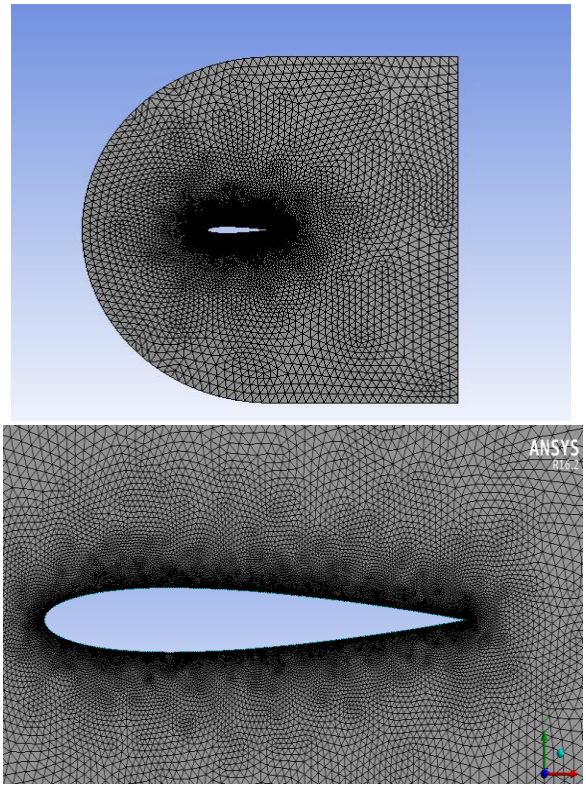

Fig. 3. (a) Mesh around NACA0012 airfoil (b) Mesh details close to airfoil.

a. Numerical Boundary and Simulation Setup

Use ANSYS Fluent 16.2 to complete the meshing part (e.g., Figure 3). Following the process of face mashing and body sizing in the mash part, we chose a coordinate name for the inlet, outlet, and airfoil along the boundary. In the setup phase, we chose a density-based solver type, a steady time interval, and a planar 2D space. Then, in the model section, we selected k-epsilon in sequential order. Standard initialization was selected as solution initialization and the data was computed from the inlet. The calculation yielded the isentropic parameters.

Table I. Simulation Reference values

Parameter	Type
Area, A	$1m^2$
Density	$1.225\ kg/m^3$
Characteristic Length	$1m$
Velocity	$2m/s$
Dynamic Viscosity	1.7894×10^{-5}

Table II. Simulation Setup Parameter

Parameter	Type
Airfoil Type	NACA 0012
Solver	Pressure based
Simulation Configuration	2D
Turbulence Model	k-ϵ Turbulence
Inlet	Velocity Inlet
Outlet	Pressure Outlet
Airfoil Wall	wall
Compute region	Inlet
Material	air
Reported Definition	Lift and Drag Coefficient

III. RESULT AND DISCUSSIONS

3.1 Lift and Drag Coefficient vs Angle of attack

In this study, we conducted a numerical analysis of NACA0012 airfoils. We calculated the lift and drag coefficients for NACA 0012 airfoils at a wind velocity of 2 m/s and angles of attack ranging from -15° to 15°. We numerically obtained the lift-and-drag coefficients using ANSYS Fluent 16.2.This work used the k-ϵ turbulence model. For NACA 0012, we gave 500 iterations, and the solution converged at 239 (Figure 4). When our angle begins at negative 15 and

stays constant at negative 10, it begins to increase until it reaches plus 10, at which point it returns to its initial value (Figure 5). However, the drag coefficient initially decreases before zero degrees and then gradually increases after that (figure 6).

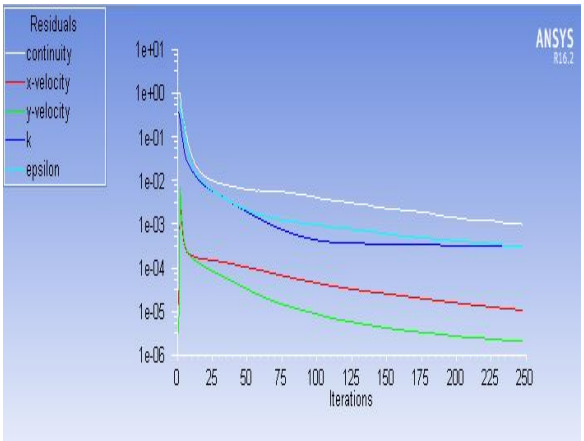

Fig. 4. Residual Convergence NACA0012

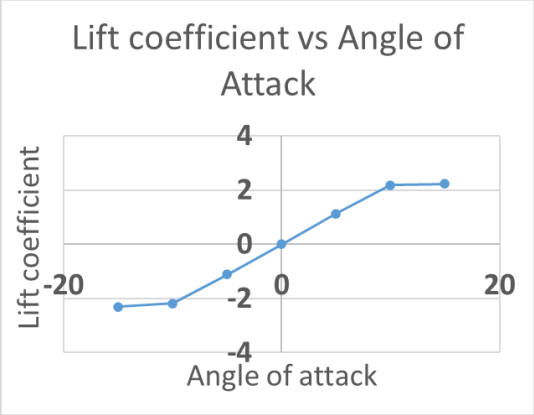

Fig. 5. Lift Coefficient vs Angle of Attack

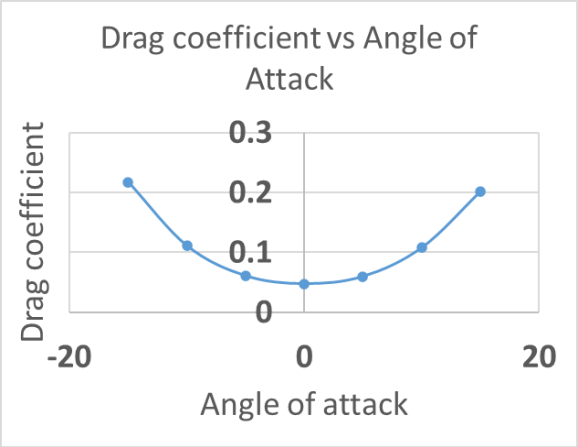

Fig. 6. Drag Coefficient vs Angle of Attack

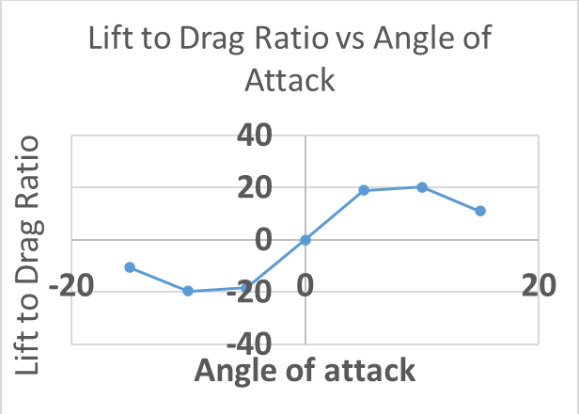

Fig. 7. Lift to Drag Ratio vs Angle of Attack

3.2 Contour of Static Pressure over a NACA 0012 airfoil

The contour of static pressure over a NACA 0012 airfoil exhibits distinct characteristics. Above the airfoil, pressure decreases sharply near the leading edge, forming a suction peak, before gradually recovering towards the trailing edge. Conversely, pressure below the airfoil increases near the leading edge, creating a region of higher pressure. As the angle of attack increases, the suction peak shifts upward and forward, intensifying the pressure gradient. At lower angles of attack, the pressure distribution becomes more uniform, with a less pronounced suction peak. This pressure contour influences the airfoil's lift and drag characteristics, making the NACA 0012 a well-studied and widely used airfoil design. See figure 8&9

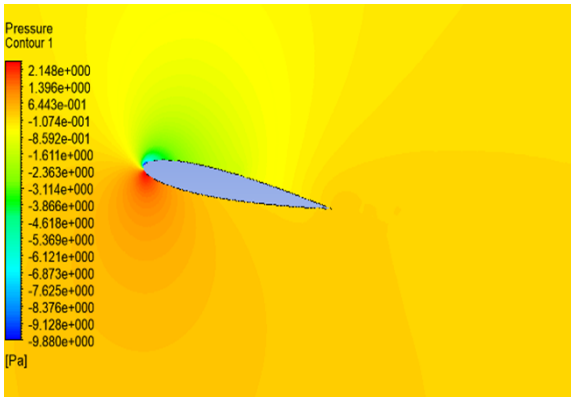

Fig. 8. Pressure Contour NACA 0012 (10° AOA)

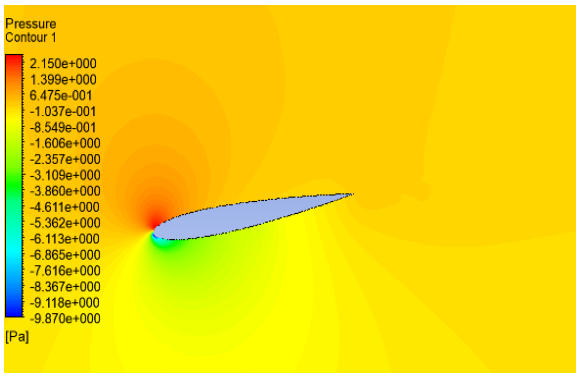

Fig. 9. Pressure Contour NACA 0012 (-10º AOA)

3.3 Contour of Static Velocity around a NACA 0012 airfoil

The contour of static velocity around a NACA 0012 airfoil exhibits distinct characteristics. Above the airfoil, velocity increases sharply near the leading edge due to the curved upper surface, reaching maximum values around mid-chord. Conversely, velocity below the airfoil remains relatively constant. As the angle of attack increases, the velocity gradient intensifies, amplifying the difference between upper and lower surface velocities. Near the trailing edge, velocity decreases, indicating flow deceleration. This velocity distribution governs the airfoil's lift and drag performance.

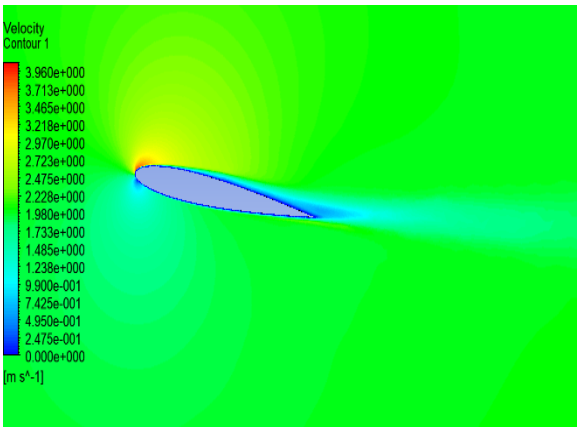

Fig. 10.Velocity Contour NACA 0012 (10º AOA)

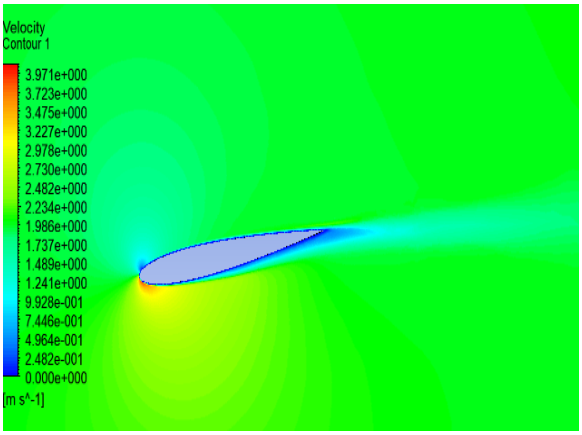

Fig. 11. Velocity Contour NACA 0012 (-10º AOA)

CONCLUSION

This project utilized CFD simulations in ANSYS Fluent to explore the aerodynamic properties of a NACA 0012 airfoil. My understanding of various angles of attack that influence the airfoil's behavior has deepened through the modeling of airflow around it. The simulations for the calculation of lift, drag, and pressure coefficients enable the identification of the stalling angle. The lift-to-drag ratio was also analyzed. The study investigates the correlation between the lift coefficient (CL) and the angles of attack, which indicates a uniform airflow without any separation. The lift coefficient varies slightly between the angles of attack of 15 and -10, increases, and then shows a slight difference between 10 and 15. The predicted drag coefficients (CD) for all angles of attack are slightly higher than the corresponding experimental data. Laminar flow in the aircraft's front section is the expected cause of this discrepancy. However, many simulations consider a completely turbulent boundary layer and the whole airfoil length. To accurately evaluate a turbulence model's performance, experimental data from a fully turbulent boundary layer is essential.

REFERENCES

[1] Achleitner, J..Rohde-Brandenburger, K.and Rogalla von Bieberstein, P,; Sturm, F.; Hornung M 2019 Aerodynamic Design of A Morphing Wing Sailplane AIAA Aviation Forum 2816

[2] Singh, I.,2017 Effect of Plain Flap Over the Aerodynamic Characteristics of Airfoil NACA

66- 015 International Journal of Innovative Science and Research Technology 2 353-365.

[3] Katz, J. and R, Largman, R., 1989 Effect of 90-Degree Flap on the Aerodynamics of a TwoElement Airfoil Journal of Fluids Engineering 111.

[4] Mahmood, Z, Khan., M, K, Scale., W, J, Bruun., H, H. 1995 Comparison of measurement and computed Transaction nce of Multi Gurney Flaps Configuration on Airfoil Engineering Research Journal (ERJ) 1 34-42.

[5] Bartlett D. W., Patterson Jr J. C., The NASA supercritical-wing technology. CTOL Transport Technol. Conf. (NASA-TM-78731) 1978.

[6] Hsiun, C. and Chen, C., 1996. Aerodynamic characteristics of a two-dimensional airfoil with ground effect. Journal of Aircraft, 33(2), pp.386-392.

[7] Barber, T. Leonard, E. and Archer, D., 1998. Appropriate CFD techniques for the prediction of ground effect aerodynamics. Proceedings of Workshop 'WISE up to ekranoplan GEMs', University of New South Wales, Sydney, Australia.

[8] Chun, H. and Chang, R., 2003. Turbulence flow simulation for wings in ground effect with two ground conditions: fixed and moving ground. International Journal of Maritime Engineering, 145, pp.51-68.

[9] Wu, C.K. and Rozhdestvensky, K.V., 2001. High-Reynoldsnumber flow computations for wings in ground effect. Proceedings of 6th International Conference on Fast Sea Transportation, Southampton, UK.

[10] Belamadi, R., Djemili, A., Ilinca, A. & Mdouki, R. Aerodynamic performance analysis of slotted airfoils for application to wind turbine blades. Journal of Wind Engineering and Industrial Aerodynamics 151, 79–99 (2016), https://doi.org/10.1016/j.jweia.2016.01.011.

[11] Beyhaghi, S. & Amano, R. S. Improvement of Aerodynamic Performance of Cambered Airfoils Using Leading-Edge Slots. Journal of Energy Resources Technology 139, (2017), https://doi.org/10.1115/1.4036047.

[12] Almusawi, M., Rishack, Q. & Al-fahham, M. Effect of Spanwise Semicircular Groove on NACA 0012 Airfoil. Basrah Journal for Engineering Sciences (BJES), 2022, 22 (2), 23–26. https://doi.org/10.33971/bjes.22.2.4.

[13] Venkatesh, D. T., Chikkanna, D. N., Basawaraj, D., Palekar, S. G. & Raikar, A. M. Design and Computational Analysis of Continuous Groove Effect on the Wing. International Research Journal of Engineering and Technology 08(10), 66, (2021), https://www.irjet.net/volume8-issue10